Automated UF$_6$ Cylinder Enrichment Assay: Status of the Hybrid Enrichment Verification Array (HEVA) Project

POTAS Phase II

David V. Jordan, Christopher R. Orton, Emily K. Mace, Benjamin S. McDonald, Jonathon A. Kulisek, L. Eric Smith

June 2012

Pacific Northwest
NATIONAL LABORATORY

This document was printed on recycled paper.
(9/2003)

Automated UF$_6$ Cylinder Enrichment Assay: Status of the Hybrid Enrichment Verification Array (HEVA) Project

David V. Jordan, Christopher R. Orton, Emily K. Mace, Benjamin S. McDonald, Jonathon A. Kulisek, L. Eric Smith[1]

June 2012

Pacific Northwest National Laboratory
Richland, Washington 99352

---

[1] Project contributions by L. Eric Smith were prior to his current IAEA appointment.

ABSTRACT

Pacific Northwest National Laboratory (PNNL) is developing a technique that will allow the International Atomic Energy Agency (IAEA) to automate UF_6 cylinder nondestructive assay (NDA) verification currently performed at enrichment plants. The IAEA has recently proposed the concept of an unattended cylinder verification station (UCVS), a concept with similarities to previous PNNL work, to positively identify each cylinder and measure its mass and enrichment. This report summarizes the status of the research and development of an enrichment assay methodology supporting the unattended cylinder verification station concept that has been ongoing for several years. The described enrichment assay approach exploits a hybrid of two passively-detected ionizing-radiation signatures: the traditional enrichment meter signature (186-keV photon peak area) and a non-traditional signature, manifested in the high-energy (3 to 8 MeV) gamma-ray continuum, generated by neutron emission from UF_6. PNNL has designed, fabricated, and field-tested several prototype assay sensor packages in an effort to demonstrate proof-of-principle for the hybrid assay approach, quantify the expected assay precision for various categories of cylinder contents, and assess the potential for unattended deployment of the technology in a portal-monitor form factor. We refer to recent sensor-package prototypes as the Hybrid Enrichment Verification Array (HEVA). The report provides an overview of the assay signatures and summarizes the results of several HEVA field measurement campaigns on populations of Type 30B UF_6 cylinders containing low-enriched uranium (LEU), natural uranium (NU), and depleted uranium (DU). Approaches to performance optimization of the assay technique via radiation transport modeling are briefly described, as are spectroscopic and data-analysis algorithms.

Contents

1.0   Introduction

International Atomic Energy Agency (IAEA) inspectors currently perform periodic inspections at uranium enrichment plants to verify UF_6 cylinder enrichment declarations. Measurements are typically performed with handheld high-resolution instruments on a statistical sampling of cylinders taken to be representative of the facility's entire product-cylinder inventory. The IAEA has recently proposed the concept of a "unattended cylinder verification station (UCVS)" as a measure to strengthen enrichment plant safeguards and reduce the amount of time that IAEA inspectors must devote to routine, on-site measurements and sample collection. A UCVS could be located at key measurement points to positively identify each cylinder, measure its mass and enrichment, store the collected data in a secure database, and maintain continuity of knowledge on measured cylinders until IAEA inspector arrival. [Smith 2012] Pacific Northwest National Laboratory (PNNL) has been working on the sensor package component of an automated cylinder verification station to enable 100 percent product-cylinder enrichment assay verification and potentially, mass-balance calculations on the facility as a whole (by also measuring feed and tails cylinders), in support of their early vision of such a station [Smith 2010b]. We refer to the PNNL-developed assay sensor package as the Hybrid Enrichment Verification Array (HEVA).

HEVA is a hybrid enrichment assay technique that combines the traditional enrichment-meter method (based on the 186 keV peak from ^{235}U) with non-traditional neutron-induced high-energy gamma-ray signatures (spawned primarily by ^{234}U alpha emissions and ^{19}F (α,n) reactions). PNNL research conducted in the 2009 to 2012 timeframe has provided proof-of-principle for the non-traditional signatures to support accurate, full-volume interrogation of the cylinder enrichment, thereby reducing the systematic uncertainties in enrichment assay due to UF_6 heterogeneity and providing greater sensitivity to material substitution scenarios [Mace 2010, Smith 2009, 2010a,b]. We have also investigated spectrum analysis techniques supporting robust, automated implementation of the traditional enrichment-meter signature. We have quantified the potential assay precision of a hybrid approach implementing both non-traditional and traditional signatures by conducting several field campaigns in which populations of UF_6 cylinders containing enriched product (2 to 5 wt%), natural uranium (NU) feed (0.71 wt%), and depleted tails (~0.2 wt%). The field campaigns have supported collection of empirical data for evaluation of the assay algorithms developed in the course of the research, and provide a performance test-bed for systematic, modeling-based design optimization of the prototype sensor package.

Results of the measurement campaigns conducted to date suggest that the hybrid assay approach comfortably meets IAEA target enrichment-assay precision values [Kuhn 2001] for 30B cylinders containing low-enriched product, NU feed, and depleted tails. No Type 48 cylinders have yet been measured. Measurement times adopted in our field campaigns are currently in the range of 5 to 10 minutes per cylinder. Counting statistical uncertainties are small compared to inherent, or systematic, variability observed over the cylinder populations assayed to date, indicating the potential for reducing these dwell times without seriously compromising precision. We are computationally assessing a set of several systematic uncertainties, including variations

in cylinder wall thickness (relevant to the traditional enrichment meter method), material age, UF_6 fill profile, isotopic composition of the feed stock (in particular, stability of the abundance ratio of ^{234}U to ^{235}U), and enrichment cascade performance. The latter two factors suggest that a facility-specific, and potentially feed-source specific, calibration may be required to achieve optimal precision with the hybrid signature methodology.

The results of this work suggest that the hybrid non-destructive analysis (NDA) method has the potential to serve as the foundation for an unattended cylinder verification station. When compared to today's handheld, attended cylinder-verification approach, such a station would have the following advantages: 1) improved enrichment assay precision for product, tail and feed cylinders; 2) full-volume assay of absolute ^{235}U mass; 3) single instrumentation design for both Type 30B and Type 48 cylinders; and 4) substantial reduction in the inspector effort associated with cylinder verification.

This report briefly summarizes the status of PNNL research on the NDA aspect of the unattended UF_6 cylinder inspection system concept. Section 2 below discusses the scientific basis of the passive gamma-ray and neutron-induced assay signatures exploited in the hybrid-assay method. Section 3 outlines modeling and sensor design considerations, with an emphasis on presenting the results of several collimation optimization studies. Section 4 focuses on the measurement campaigns conducted by PNNL at the AREVA enrichment plant in Richland, WA, U.S.A. We present the assay results, quantified in terms of the relative assay precision for various assay algorithms applied to several populations of product cylinders. Analysis methods relevant to the field campaign data reduction are described briefly in an Appendix (Section 6). Section 5 summarizes the research to date and indicates directions for future work.

2.0 UF_6 Cylinder Enrichment Assay Signatures

This research addresses assay of uranium enrichment in UF_6 cylinders via passive detection of gamma-ray and/or neutron emissions. Natural UF_6, known as *feed,* as well as *tails* material (UF_6 depleted in ^{235}U), is handled in 48" (122 cm)-diameter cylinders. Enriched UF_6, called *product*, is handled in smaller, 30" (76 cm)-diameter cylinders designated Model 30B (Figure 1). Product material is more sensitive than tails or feed from a proliferation standpoint; and product cylinders are separately routed.
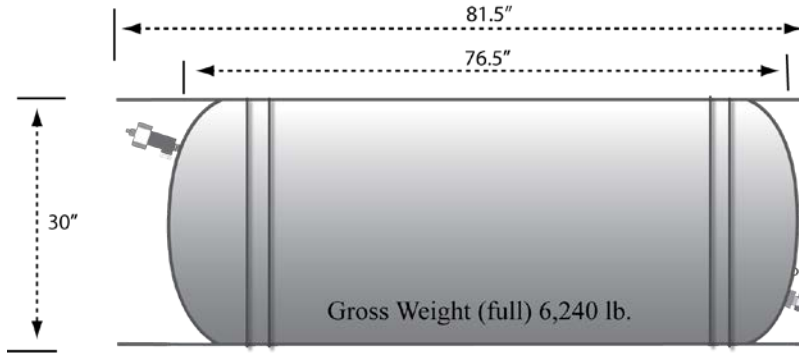
Figure 1: 30B Cylinder Dimensions

Several ionizing-radiation emission signatures are of potential utility for enrichment assay of UF_6 cylinders; see Figure 2. The *traditional* enrichment meter method involves analysis of the 186-keV emission line intensity and provides a direct measure of the U-235 abundance in a relatively small volume of the inspected cylinder. The accuracy and precision of the traditional approach depend upon the gamma-ray sensor system, the configuration of UF_6 in the cylinder interior (including possible deposition on the cylinder wall), and wall thickness variations over a given population of cylinders. Current IAEA inspector-based assay procedure involves application of portable, high-resolution spectrometers (i.e. HPGe) to implement the enrichment meter method. The present research is assessing the application of *medium-resolution* scintillators, rather than HPGe, to measurement of both traditional and non-traditional signatures (discussed below). In contrast to the present operational model of inspector-attended measurements, the scintillation spectrometers would be deployed in an unattended sensor package installed at a fixed "portal monitor" location in the cylinder process stream. While the energy resolution of these medium-resolution scintillators is inferior to that of HPGe, it is still adequate to quantify the net number of counts in the 186-keV peak. For example, previous work by other groups has shown that NaI-based 186-keV peak analysis, using a collimated handheld device and measurements at a single location on the cylinder, can achieve approximately 5% uncertainty for product cylinders [Walton 1974, Dias 2008].   A hypothesis of the UCVS concept is that a fixed-geometry instrument that utilizes an array of spectrometers can reduce systematic uncertainties due to wall thickness variations and UF_6 heterogeneity in the cylinder, and that proper collimation and shielding of the spectrometers can improve robustness against potentially time-varying facility background (arising from, e.g., changes in the physical locations of nearby cylinders).

1. Traditional 186-keV region of interest
   Direct measure of ^{235}U, but weakly penetrating
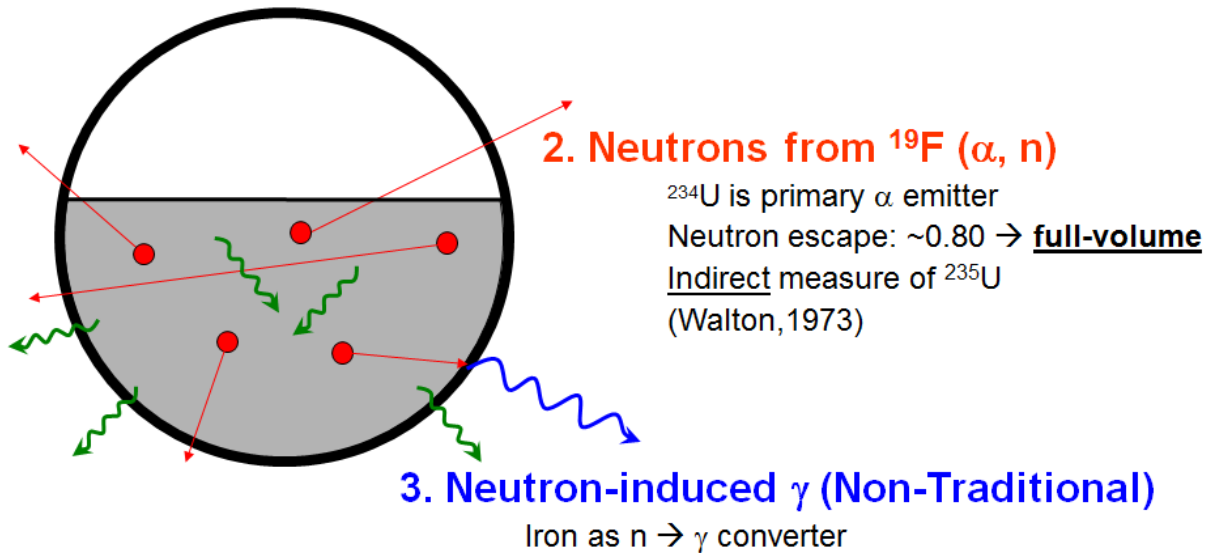   NaI-based measurements ~5% uncertainty on product (Walton, 1973)

2. Neutrons from ^{19}F (α, n)
   ^{234}U is primary α emitter
   Neutron escape: ~0.80 → **full-volume**
   Indirect measure of ^{235}U
   (Walton,1973)

3. Neutron-induced γ (Non-Traditional)
   Iron as n → γ converter

Figure 2. Schematic depiction of several ionizing-radiation assay signatures from UF$_6$ cylinders.

Non-traditional assay exploits passive detection of neutrons emitted from UF$_6$, either directly (via a neutron sensor) or indirectly (via detection of neutron capture gamma-rays emitted from structures proximate to the UF6). The potential use of gross-counting neutron detection as a means of determining UF$_6$ enrichment has been studied previously [Walton 1974, Reilly 1974] but is not currently used in IAEA verification measurements. The neutron signature is attractive because of the high penetrability of neutrons from the interior of the cylinder volume to the outside wall. The fraction of neutrons escaping the cylinder wall ranged from 0.80 to 0.90 in previous studies [Walton 1974], with weak dependence on the cylinder enrichment and fill level. The primary source of neutrons from product cylinders is F-19(α,n) reactions, with the dominant alpha emitter being U-234 for all enrichments above natural. Sources of neutrons other than U-234 include U-238 spontaneous fission and alpha emission, and induced fission in U-235.

Exploiting the neutron yield as an indirect measure of U-235 requires stability of the U-234/U-235 ratio over the population of product cylinders subjected to assay. Work by Richter et al. [1999] assessing global variations in NU composition suggests a dispersion on the order of 5% in the relative U-234 isotopic abundance. Because the F-19(α,n) yield is essentially proportional to the U-234 abundance for low-enriched product, this variability would in turn induce about 5% variability in the non-traditional signature yield at fixed enrichment. Other studies have indicated that the isotopic ratio in the product stream may vary significantly with enrichment process, particularly for enrichments above 5% [Reilly 1974,1991]. Modern enrichment plants, depending on the price of uranium, may also recycle tails as feed material, with potential impacts on the U-234/U-235 ratio in the product cylinders. Yet another potential source of variation in this ratio is the use of reactor-recycled uranium. Thus a facility-specific calibration, and potentially a feed-stock specific calibration, might be required in order to meet IAEA enrichment

assay precision targets by using this signature of U-234 content as an indirect measure of U-235 content.

The neutron signature can in principle be measured either directly, i.e. with a neutron sensor, or indirectly, by detecting high-energy gamma-rays produced by the neutrons as they interact with the environment of the UF_6. Neutrons produced in the UF_6 interact in the UF_6 itself, the surrounding steel cylinder and adjacent structural materials, materials in close proximity to gamma-ray spectrometers, and in the scintillation spectrometers themselves. Those interactions (e.g. inelastic scatter and neutron capture) can induce high-energy gamma-ray signatures that extend to energies greater than 10 MeV. Prominent among these, due to the large volume of steel in the cylinder assay scenario, are the 7.631-MeV and 7.645-MeV lines from neutron capture reactions on Fe-56.[2] Thus the steel wall of the cylinder and steel (or other materials) located near the gamma-ray spectrometers, including collimation optimized for this purpose, can serve as neutron-to-gamma-ray converters. This high-energy gamma-ray signature is attractive from the cylinder verification standpoint for several reasons:

- It allows exploitation of a neutron signature without dedicated neutron sensors, thereby simplifying system design and reducing cost—particularly advantageous with the current shortage of He-3.
- The goal of full-volume assay is achieved by virtue of the penetrability of the neutrons (escape fraction from the UF_6 volume of greater than 80%) that induce the gamma rays.
- The high-energy gamma-ray signature is well above the energy range of copious emissions from UF_6 (e.g. 1001 keV from the Pa-234m daughter of U-238 and 2614 keV from Tl-208, daughter of U-232) and the vast majority of terrestrial gamma-ray background emissions (e.g. 2614 keV from Tl-208, daughter of Th-232).

The present research emphasizes a dual-signature approach that combines both traditional and non-traditional assay signatures in a hybrid algorithm. A hybrid assay method may be advantageous for three reasons. First, we hypothesize that an appropriately-calibrated hybrid enrichment assay method can achieve lower uncertainties than either the traditional or non-traditional methods acting independently because there is a low degree of correlation between the two predominant sources of systematic error in the two individual methods (wall thickness variation and $^{234}U/^{235}U$ variation, respectively). Random variations in signature intensity arising from these two independent sources of uncertainty will thus tend to cancel each other out, on average, over a population of inspected cylinders. Secondly, the two signatures are derived from separate detectors, separate portions of the gamma-ray spectrum (when an indirect, gamma-ray measure of the neutron-induced signature is exploited), or both. Combining the statistically-independent spectrum yields reduces counting-statistical uncertainties in the hybrid signature relative to either signature independently, thus reducing the dwell time required for a statistically-robust measurement. To date, we have only tested a simple arithmetic average of the two assay signatures, but more sophisticated approaches (e.g. with unequal weighting for the two contributions) can be envisioned. Finally, the use of a hybrid approach that combines a gamma-

---

[2] The 7.631-MeV gamma ray is the most intense line following neutron capture on Fe-56. The intensity of the 7.645-MeV line is about 86% that of the 7.631-MeV line.

origin signal with a neutron-origin signal will increase the technique's resistance to spoofing scenarios.

3.0 Sensor Design and Signature Modeling

The design of the HEVA system is influenced by the simultaneous requirements of good energy resolution for 186 keV gamma rays, good neutron capture/conversion efficiency, and good detection efficiency for the high-energy (3 to 8.5 MeV) capture gamma-rays. Large NaI detectors have good efficiency for the high-energy, non-traditional enrichment signature, but relatively poor energy resolution for the traditional enrichment meter method. Smaller detectors in cylindrical form-factor may offer better energy resolution on average compared to NaI logs (due to factors such as reduced dispersion in scintillation photon collection efficiency as a function of position in the detector), but at the cost of lower efficiency for detecting the high-energy photons. An array of cylindrical 7.6 cm × 7.6 cm NaI detectors inside of neutron-converting collimators was chosen to provide efficiency for both signals and to facilitate sampling along the length of the UF_6 cylinder. Polyethylene sheets (2.5 cm thickness) help moderate and reflect neutrons emitted from the cylinder toward the detectors and conversion collimators. The following sections present a brief description of the detector modeling and design results. We also discuss a modeling-based assessment of systematic uncertainties in the enrichment assay using the hybrid signature approach.

Models Developed to Guide System Design

Models of the 30B cylinder, detectors and surrounding geometry were created with MCNP5/X to guide the design of conversion collimators and the polyethylene neutron-reflector fences. Figure 3 shows a visualization of a configuration with 7.6 cm × 7.6 cm NaI spectrometers. To create synthetic UF_6 spectra, we generated energy distributions for the photon and neutron emissions from each uranium isotope present in the UF_6. The direct-decay gamma-ray distributions were calculated with the spectrum synthesis code, SYNTH [Hensley 2006], and the neutron emissions with the code Sources 4C [Wilson 2005]. We generated MCNP5 photon pulse-height tallies for each source term. For the neutron sources, gamma-ray emissions from both neutron-capture and inelastic scatter reactions contribute to the pulse-height tally. We can then approximate the pulse-height response for an arbitrary isotopic composition of the UF_6 contents by linear superposition of the separate isotopic responses. (Nonlinear yield effects induced by e.g. isotopic-abundance dependent interactions of fast neutrons inside the UF_6 volume are neglected in this computational procedure. We have verified that this approximation is reasonable over the range of LEU enrichments of primary concern to the project.) Figure 4 shows an example synthetic spectrum with the various response contributions isolated. Figure 5 compares measured and simulated spectra for an enrichment close to 5 wt% ^{235}U. Early incarnations of the model underpredicted the measured spectral continuum by roughly a factor

6

of two. Adding a source term to account for bremsstrahlung photons generated by beta decay of ^{234m}Pa (a ^{238}U daughter) substantially improved the model fidelity, reducing the undershoot to roughly 20% in the lower energy (<600 keV) portion of the spectrum.
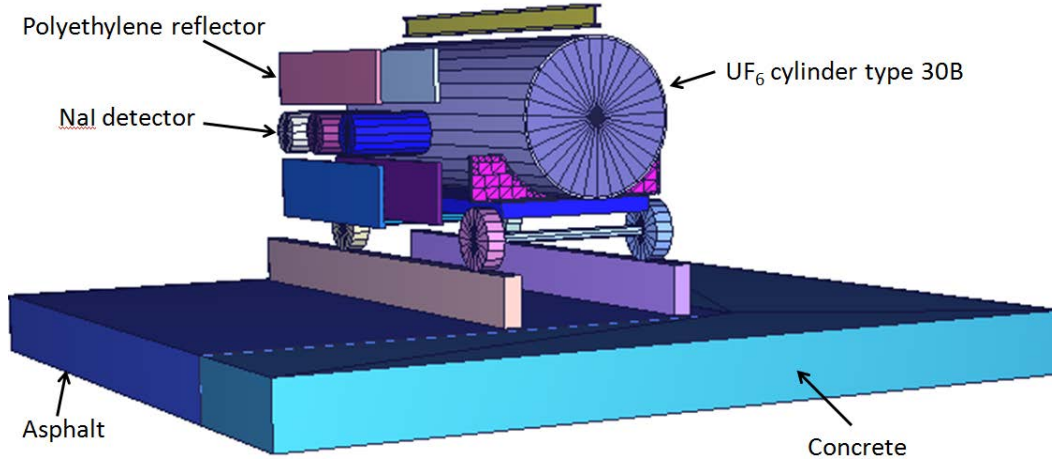

Figure 3. Visualization of an MCNP model of the 30B cylinder measurement with three NaI detectors, collimators and poly fences.
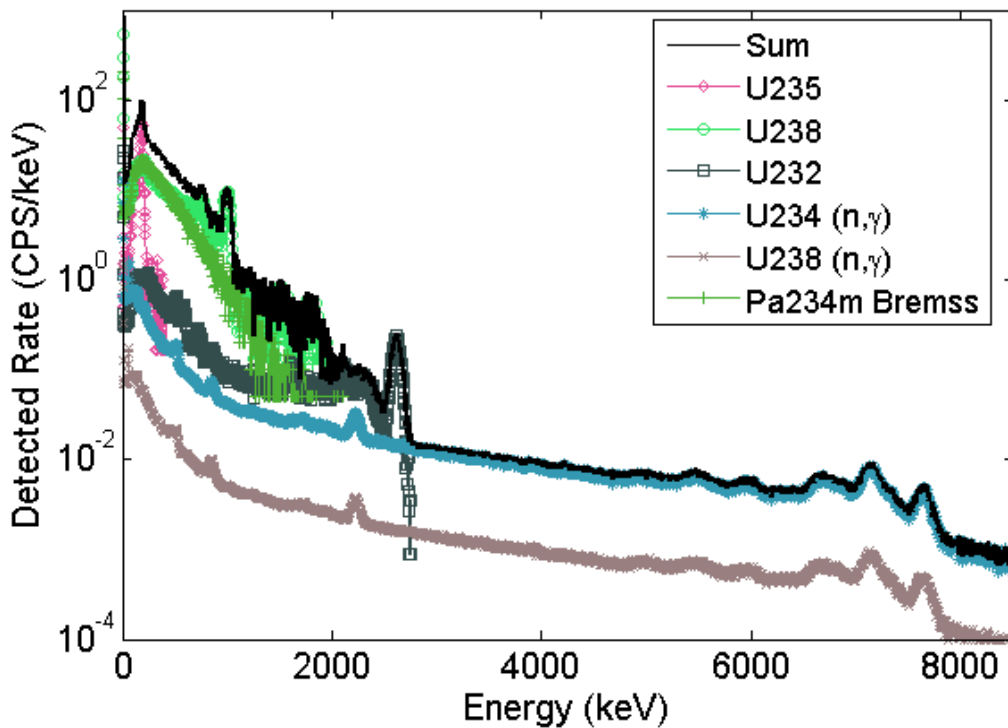

Figure 4. Simulated energy-deposition spectrum components in an NaI spectrometer viewing UF$_6$ at 4.0 wt% ^{235}U contained in a 30B cylinder.
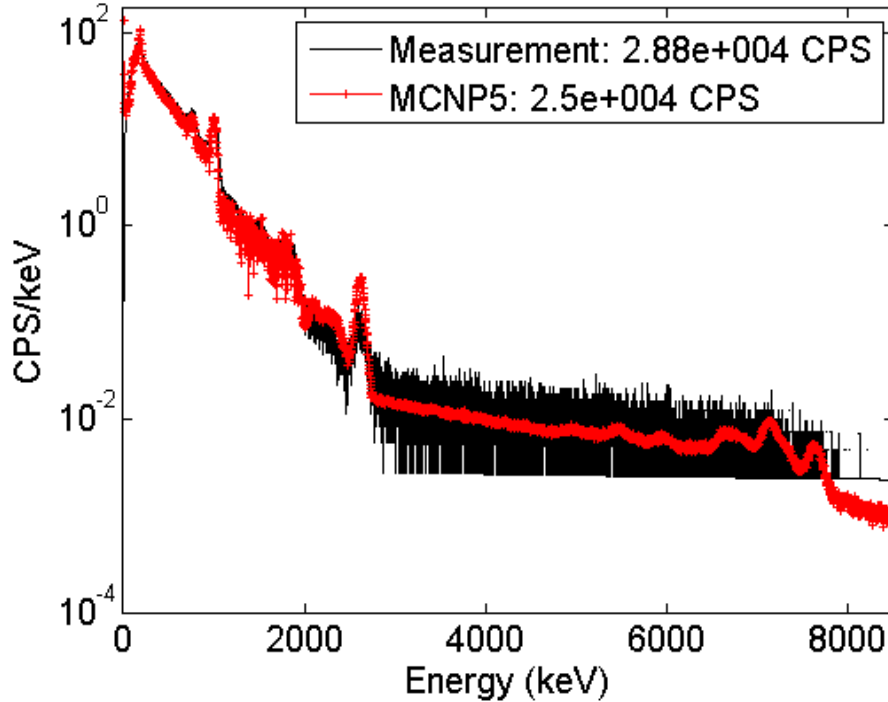
Figure 5. Comparison of measured and simulated spectra for a 4.9 wt% ^{235}U 30B cylinder.

Collimator Design and Description of Current Sensor Array

Collimators around the scintillation spectrometers serve a dual purpose: (1) For the traditional enrichment meter method, the collimators attenuate low-energy gamma-rays from portions of the inspected cylinder not falling within the geometrical field-of-view of the spectrometer, to present a well-defined sampling volume and minimize continuum background under the 186-keV peak. (2) For the non-traditional signature, the collimators moderate and/or capture neutrons such that they generate high-energy gamma-rays (above 3 MeV) as copiously as possible in the spectrometer. Designs investigated in this research and in the literature have focused on alternating layers of polyethylene and steel. Multi-layered (up to 10) configurations developed by Mitchell et al. [2010] at Sandia National Laboratory were initially investigated. Interestingly, a bi-layered approach works nearly as well as the multi-layer designs with thinner layers. However, the order of the two-layer collimator has a large effect: poly on the outside of the sandwich results in many fewer detected 3.0-8.5 MeV gamma-rays than if steel is on the outside. The spatial ordering of the layers is significant because of the two contributing physical effects of (a) the moderation and reflection of the incident neutron flux by the poly, and (b) the geometrical efficiency for capture gamma-ray collection by the NaI crystal as a function of position of the gamma-ray emission. Modeling conducted to date indicates that positioning the moderating layer *beneath* an outer steel sheath dramatically favors efficiency of capture gamma-ray detection. Figure 6 shows results for several configurations investigated. The final design was chosen to satisfy the competing constraints of (1) maximizing the 3-8.5 MeV signal, (2)

8

minimizing complexity and cost of construction, and (3) minimizing mechanical support requirements for deployment of the HEVA sensor package in further proof-of-concept measurement campaigns. The final collimator design is depicted in Figure 7. Each collimator is approximately 18 cm long and 25 kg in mass. Increasing the length, and corresponding mass, of the collimator by about 25% increases the modeled nontraditional signal strength by less than 5%.   More detail is provided in [McDonald 2011]. Four cylindrical NaI detectors with these collimators spaced 38 cm apart comprise the latest system (currently being fabricated in FY-2012).
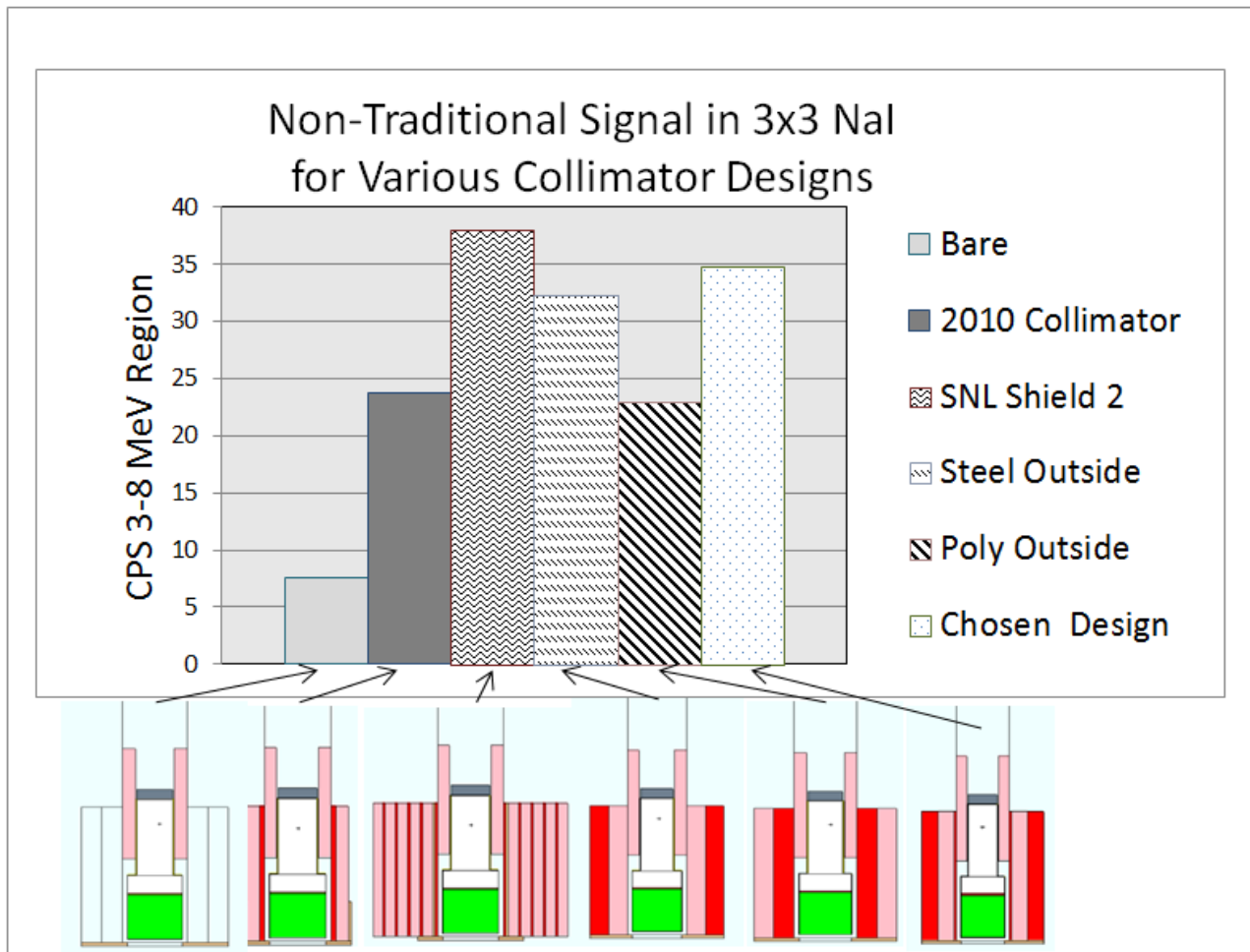

Figure 6. Modeled gamma-ray count rate over 3-8.5 MeV in a 7.6 cm × 7.6 cm NaI detector from ^{234}U neutrons for several collimator designs and a fixed 5 wt% UF$_6$ 30B cylinder. Cross-sectional views through collimator designs are shown below the chart (Pink=poly, red=steel, green=NaI) [Mitchell 2010]

In addition to optimizing the collimator design, we also applied modeling to an investigation of the optimum number and position of the poly fences. The dimensions of each fence segment are $120 \times 30 \times 2.5$ cm^3. These fences help reflect neutrons back toward the UF$_6$ cylinder or spectrometer collimator. A single front fence (set of two segments) results in as much as a 20% increase in the 3-8.5 MeV photon count rate. An additional fence placed in back of the detectors can increase the high-energy count rate by another 10%. So after the spectrometer collimators, the fences make the largest difference in the non-traditional signal strength. Figure 3 shows the two planes of fences used in the May 2011 AREVA measurement campaign, described further in section 4 below.
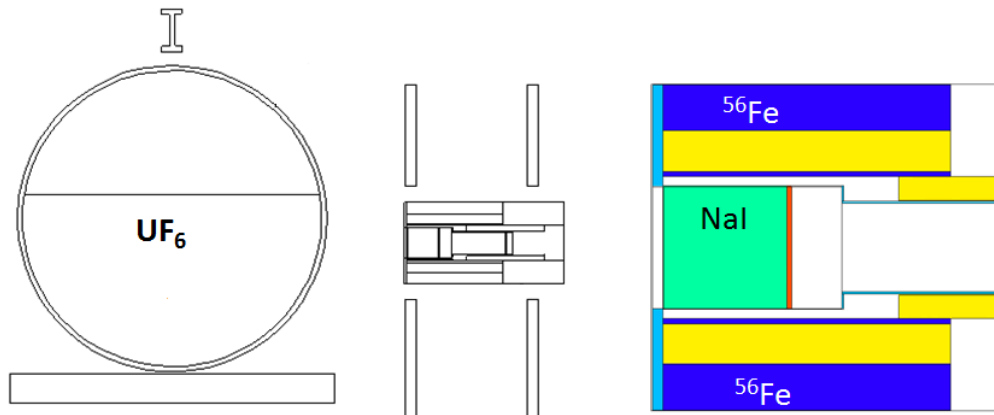

Figure 7. Illustration of the final spectrometer collimator design (right) and cross-sectional view of typical measurement geometry (left). Polyethylene is colored yellow in the collimator illustration.

Investigation of Neutron-Response Contributions to High-Energy Gamma-Ray Signature

Modeling-based investigations of the spatial distribution of (n, γ) reaction sites contributing to the high-energy signature region, and the continuum are underway. These studies are useful for determining the relative importance of structural materials, collimation, and the gamma-ray spectrometers themselves as neutron to gamma-ray converters. We are addressing this issue by studying the relative contributions of total counts to the various energy regions of the HEVA NaI detector spectra as calculated using MCNPX. Preliminary results suggest that ^{127}I in the NaI spectrometers contributes a substantial portion of the yield in each of the spectral energy regions, which is physically plausible, owing to its comparatively large (n, γ) cross section across a wide range of incident neutron energies. ^{56}Fe gamma rays external to the detectors along with ^{127}I and ^{23}Na gamma rays induced by neutrons within the NaI detectors account for almost all of the modeled response in the high-energy gamma-ray signature region. It was also determined that most of the neutron-induced gamma-rays from these isotopes were induced by (n, γ) reactions, particularly in the high-energy signature region. Contributions to the high-energy signature from neutron interactions other than (n, γ) with ^{56}Fe, ^{127}I, and ^{23}Na nuclei (e.g. neutron inelastic scattering) were negligible.

We have also used the neutron-response simulations to estimate damage to the NaI detectors arising from the neutron field. The effective lifetime of the detectors as limited by neutron-induced damage is of order 10^6 years according to these simulations. Thus the longevity and robustness of the spectrometer array under typical deployment conditions will likely be determined by environmental factors (e.g. temperature variations) rather than radiological exposure.

4.0   Field Work and Results

PNNL has performed several cylinder measurement campaigns at an AREVA NP fuel fabrication plant in Richland, Washington. The campaigns have supported proof-of-principle demonstrations of the utility of the various enrichment assay signatures and provided empirical data useful for investigation and optimization of analysis algorithms. We have tested several modifications of the sensor package. Table 4-1 below summarizes properties of the cylinder populations subjected to assay in the various campaigns. A brief description of the sensor packages, primary measurement objectives, and results follow.

Table 4-1. Summary of PNNL measurement campaigns at AREVA.

Date	No. of Cylinders				Live Time Per Cylinder (minutes)	Standoff (cm)	Instrument Package
	Total	Product (2 to 5 wt%)	Feed	Depleted			
July 3, 2008	2	2	0	0	20	160	Various
April 9, 2009	23	19	3	1	5	150	Prototype #1
April 22, 2010	26	23	2	1	5 (NaI), 6.7 (LaBr$_3$)	9.0	Prototype #2a
May 6, 2010	26	23	2	1	5 (NaI), 6.7 (LaBr$_3$)	9.0	Prototype #2b
May 19, 2011	18	12	6	0	10	22	Prototype #3

July 2008

This early measurement campaign focused on initial characterization of gamma-ray backgrounds in the vicinity of 30B cylinders and empirical confirmation of the expected proportionality between cylinder enrichment and the neutron signature. Both gamma-ray and neutron sensors were deployed. In contrast to later campaigns, the sensor package had been previously designed and fabricated for another project. Detailed measurements were taken on a full URENCO cylinder containing non-recycled uranium, a Russian down-blended cylinder with recycled uranium, and an empty cylinder with heels. Background measurements were taken at two

different locations. Measurements were taken with an Ortec Detective®, an Exploranium GR-135®, and a miniature version of the portal monitor enrichment panel containing three NaI detectors and eight, moderated ^{3}He detectors.

Figure 9 and Figure 10 display key results from this initial characterization campaign. Net neutron count rates (Figure 9) suggested that the expected correlation between ^{234}U and ^{235}U mass may be realized. The heels cylinder that was measured held ~0.038 kg of ^{235}U , the standard-enriched cylinder ~71.1 kg, and the down-blended cylinder ~65.9 kg. The neutron count rates (from 1.6 m away) for the down-blended and standard-enriched cylinder were consistent in terms of proportionality to ^{235}U mass. Gamma ray spectroscopy of these same cylinders, using large-volume NaI spectrometers, showed a relationship that corroborates the neutron analysis when correlating ^{235}U mass and high-energy count rates in the 4–7 MeV range (Figure 10).

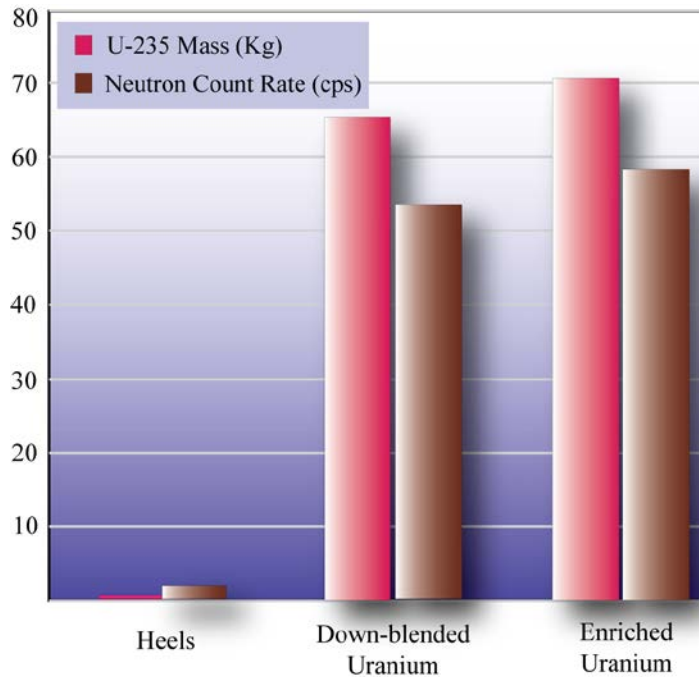**Figure 8. AREVA NP Measurements Indicating Correlation between Neutron Counts and ^{235}U**
 (It is notable that although the heels-cylinder ^{235}U mass (0.038 kg) is too low to be seen on
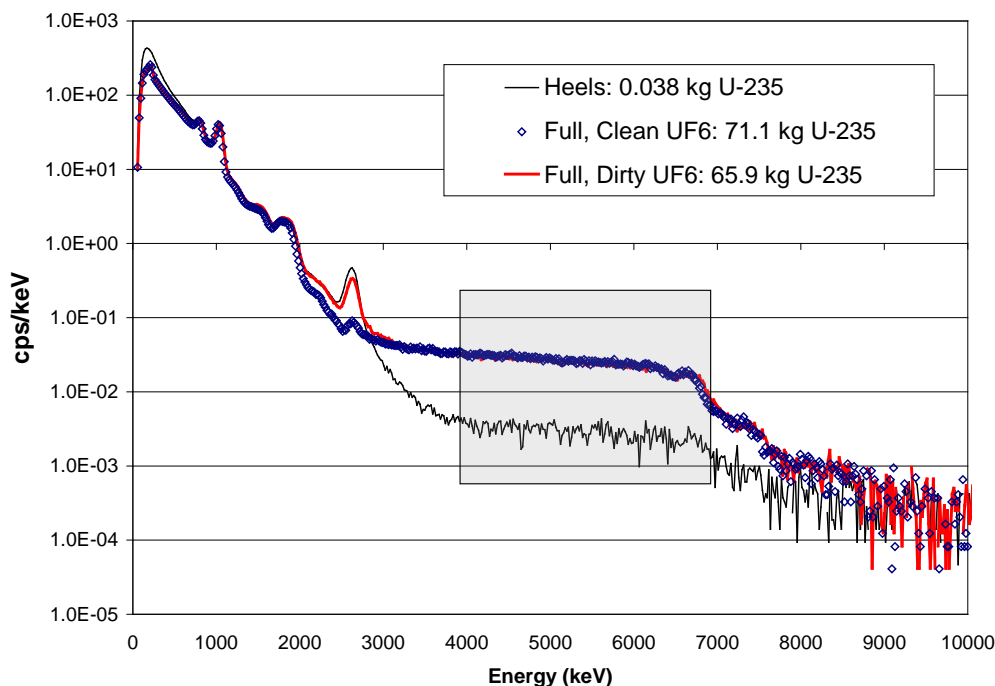 this plot, the neutron count rate is appreciable.)

Figure 9. AREVA NP Correlation between High-Energy Gammas and ^{235}U Mass

April 2009

Following the promising characterization measurements in 2008, which focused on a small set of cylinders, PNNL deployed a custom-designed instrumentation package in a second field campaign at AREVA that measured a more extensive population (23) of cylinders. The enrichment-assay portal comprised both gamma-ray and neutron sensors. The primary measurement objectives were to (a) test linearity of the neutron signature as a function of U-235 mass, (b) compare direct neutron-sensor and indirect, neutron-induced, high-energy gamma-ray sensor responses, and (c) assess potential assay precision achievable with the direct and indirect neutron signatures, and compare this precision to that achieved via the enrichment meter method with high-resolution gamma-ray. PNNL developed a sensor package (referred to herein as "Prototype #1" in Table 4-1 above; see Figure 11) that included two log-shaped NaI spectrometers ($10 \times 10 \times 40$ cm^3 and $10 \times 5 \times 20$ cm^3) and a set of four He-3 tubes in a polyethylene moderator matrix. The package included gamma-ray shielding (1.0 cm of steel on the sides, 2.5 cm on bottom and back) and neutron shielding (5 cm of 5% borated polyethylene on 5 sides) to improve background rejection. The sensor system also included a dedicated data acquisition system, a lift to allow variation in vertical position, and a hand-truck-like chassis to allow the system to be moved through standard doorways. The hand-truck form factor proved adequate for proof-of-principle measurements of the neutron-related signatures, but it was not appropriate for a demonstration prototype that also uses the traditional 186-keV enrichment meter measurement. (PNNL subsequently designed and fabricated a modified prototype system, Prototype #2, that included collimated NaI(Tl) and LaBr$_3$(Ce) sensors in close proximity to the

cylinder wall; see sub-section "April and May 2010" below.)   Figure 12 displays a photograph of the sensor geometry for a typical cylinder measurement at AREVA. Measurement live times were 300 seconds per cylinder.

Figure 13 through Figure 15 display results for the neutron and high-energy gamma-ray signatures. A malfunction of the neutron sensor's data acquisition system limited useful data collection for that signature to only 11 product cylinders. Assuming stability of the U-234/U-235 ratio over this set of cylinders, the relationship between intensity of the neutron signature and the U-235 mass should be linear. A linear fit to the observed neutron intensity as a function of U-235 mass supports the hypothesis of this isotopic abundance stability (Figure 13). The calibration determined from this linear fit yields a relative standard deviation of assayed U-235 mass from the declared values of 5.2% when applied to this enriched-product cylinder population. Results for the high-energy gamma-ray region are shown in Figure 14 and Figure 15. The net high-energy count rate from 22 cylinders, 19 of which were product cylinders, is plotted against U-235 mass. Consistent with the neutron-signature assay results, the hypothesis of a stable U-234/U-235 ratio is again supported by the linear relationship. The relative standard deviation of those measurements from the declared U-235 mass is 6.4%.   Note that this procedure for evaluating the assay precision assumes the uncertainties in the facility-declared enrichments are small compared to the NDA uncertainties. In principle, the declared enrichment values (and U-235 masses derived from these declarations) have a finite uncertainty associated with them which are representative of whatever methods have been used at the relevant enrichment facility to characterize product enrichment (e.g. physical sampling of the product stream and subsequent mass spectrometric analysis). We have neglected these declaration uncertainties in all analyses of field campaign results to date.
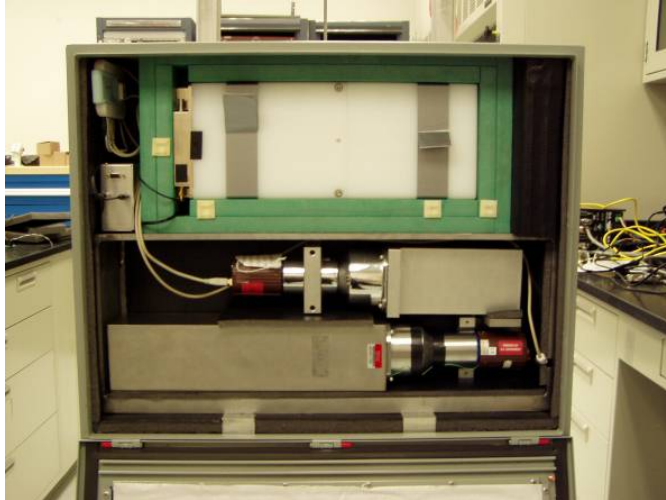
Figure 10. Proof-of-principle sensor package ("Prototype #1") deployed in April 2009 AREVA field campaign. The sensor package consists of a 4-tube moderated He-3 module (white) with borated poly shielding (green); at the bottom of the sensor panel are two large NaI(Tl) spectrometers (10×10×40 cm and 10×5×20 cm).

Figure 11. Experimental setup at AREVA fuel fabrication facility for the April 2009 field campaign. The proof-of-principle NaI/He-3 panel and a 120% HPGe spectrometer are at left, approximately 1.5 m from the cylinder wall. At right, a cylinder is lowered onto a trolley.
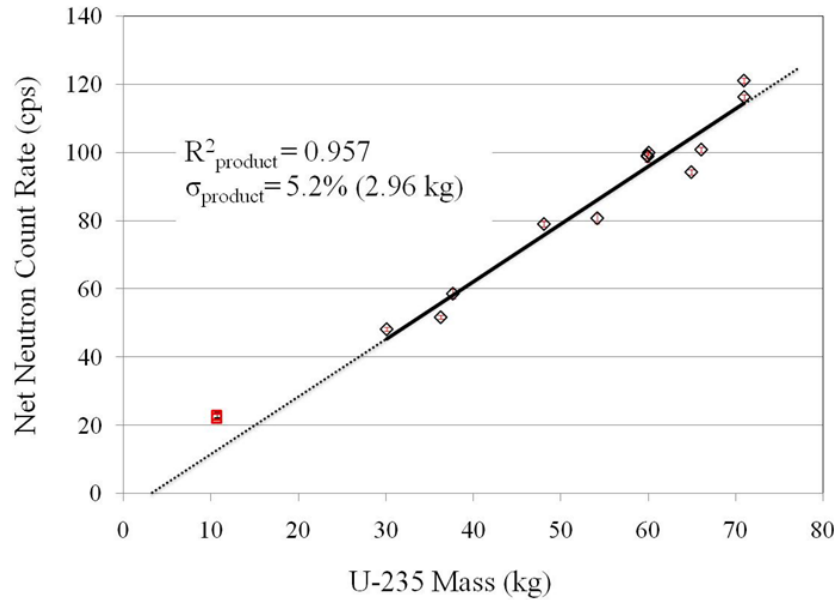
Figure 12. Net neutron count rate versus U-235 mass for 11 product cylinders in the April 2009 AREVA field campaign. Natural and depleted cylinders (red boxes below 15 kg of U-235) are shown, but were excluded in the fit. Statistical counting uncertainty is indicated by the red error bars (typically smaller than the dimension of the diamond-shaped markers).

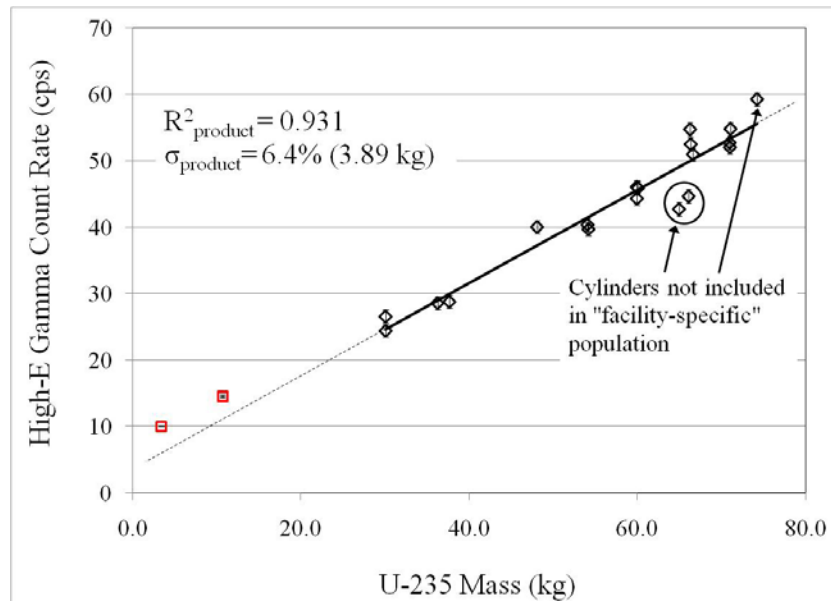**Figure 13. Net high-energy gamma count rate (in a window spanning 3.0 MeV to 8.0 MeV) versus U-235 mass for 19 product cylinders (all suppliers/processes) in the April 2009 AREVA field campaign. Natural and depleted cylinders (red boxes below 15 kg of U-235) are shown, but were excluded in the fit. Statistical counting uncertainty is indicated by the error bars, generally smaller than the diamond-shaped markers.**

As discussed in Section 2 above, variation in both feed material composition and enrichment processes can impact the product U-234/U-235 ratio. It is expected, therefore, that a facility-specific calibration will be needed to mitigate systematic uncertainties in that ratio and the U-234-derived neutron and high-energy gamma-ray signatures. To test this assertion, 3 of the 19 product cylinders included in the high-energy gamma analysis (Figure 14) were removed from the population: one documented as HEU-downblend material, and two from a Russian enrichment facility called Ural Electrochemical Integrated Plant, which is also reported to be processing HEU-downblend material. The remaining 16 cylinders are from either USEC or URENCO and are taken to represent the kind of population that might be produced by a single facility. Such a "facility-specific" calibration is shown in Figure 15. Removal of the cylinders known to be produced from different feed or enrichment processes has a marked effect on the relative standard deviation, which is now reduced to 4.7% from the declared U-235 mass.

$R^2_{product} = 0.971$
$\sigma_{product} = 4.7\% \ (2.51kg)$
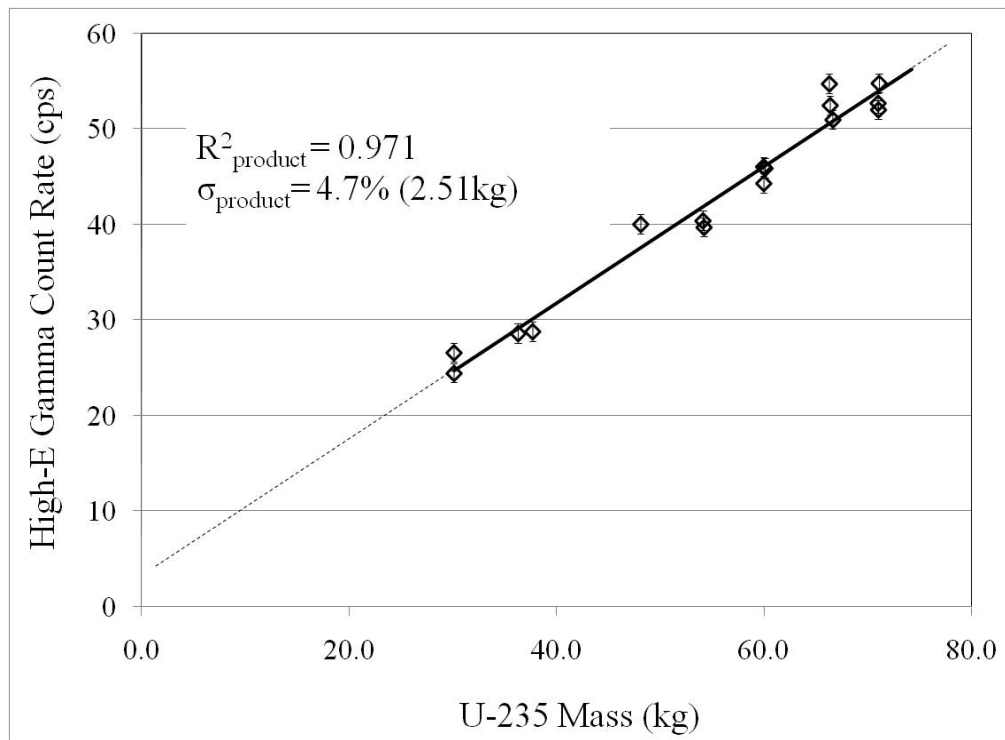
Figure 14. Net high-energy gamma count rate versus U-235 mass for the 16 product cylinders from either URENCO or USEC, April 2009 AREVA field campaign. Statistical counting uncertainty is indicated by the error bars, generally smaller than the dimension of the diamond-shaped markers

Table 4-2 summarizes the April 2009 proof-of-principle measurements and subsequent analysis of cylinder assay utilizing the non-traditional (i.e. neutron and high-energy gamma-ray) and traditional signatures (based upon AREVA HPGe assay).

Table 4-2. Summary of enrichment assay results for 30B product cylinders (enrichment ranging from 2% to 4.95%), AREVA April 2009 measurement campaign.

Method	Product	#Cylinder
Approximate Target Uncertainty [Kuhn 2001][3]	**5**	**---**
Traditional HPGe (from AREVA)	**4.3**	**16**
Non-Traditional NaI High-E gamma	4.7	16
Hybrid Non-Traditional + AREVA Traditional HPGe (simple average)	3.6	16
Total neutron	5.2	11

April and May 2010

PNNL conducted two sets of measurements at AREVA in 2010 using a sensor package in two different collimation configurations ("Prototype #2a and 2b") comprising gamma-ray spectrometers only. The primary goals of these campaigns were to (a) test the precision of a non-traditional (i.e. neutron-induced) assay methodology based solely upon the high-energy gamma-ray response, rather than a direct neutron-sensor measurement, (b) examine the traditional, enrichment-meter assay precision achievable as a function of energy resolution in the 186-keV peak region, by using two different gamma-ray spectrometers at moderate (~6.5% at 662 keV for NaI) and good (2.4% at 662 keV for LaBr$_3$) energy resolution, and (c) explore hybrid assay algorithms incorporating both non-traditional and traditional assay signatures (the latter measured via medium-resolution scintillation spectrometer, as opposed to the HPGe assay used to construct the hybrid signature in the April 2009 field campaign). The sensor set (see Figure 16) included two NaI spectrometers (one cylindrical, 7.5 cm diameter × 7.5 cm long, and one log, 10×5×20 cm^3) and one LaBr$_3$ spectrometer (cylindrical, 3.8 cm diameter × 3.8 cm long). The two campaigns incorporated two different collimation designs, in order to address the following research questions:

1. What traditional-assay performance can be realized with a collimator design ("Prototype #2a") focused on collecting only the low-energy signatures? For these measurements and analysis, we surrounded the two cylindrical spectrometers with cylindrical lead collimators of wall thickness 2.2 cm and aperture diameters 5.1 cm and 7.6 cm for the (3.8 cm × 3.8 cm) LaBr$_3$ and (7.6 × 7.6 cm) NaI, respectively.

2. What traditional-assay performance can be realized with a collimator design ("Prototype #2b") focused on collecting and enhancing the non-traditional high-energy gamma-ray signatures? For these measurements and analysis, we surrounded the two spectrometers with cylindrical collimators consisting of 0.64 cm of steel and 1.28 cm of polyethylene.

---

[3] The target uncertainties are estimated from the combination of systematic and random errors given in Kuhn and should be used only to set the scale of the target uncertainties.

This collimator design is intended to enhance the high-energy gamma-ray signature by moderating neutrons in the vicinity of the detector and providing an iron conversion layer. This collimator also included a lead aperture on the front face (0.64-cm thick) and 0.32-cm lead wrapped around the outside of the polyethylene. This lead structure provides substantial collimation of the 186-keV (less than 0.1% uncollided penetration through 0.64 cm of lead) while minimizing the attenuation of the 7.6-MeV gamma rays (less than 3% attenuation at 0.64 cm). The lead aperture diameters were 5.1 cm, and 7.6 cm for the (3.8 cm × 3.8 cm) $LaBr_3$ and (7.6 × 7.6 cm) NaI, respectively.

In addition to the 26-cylinder population indicated for these campaigns in Table 4-1, we also measured several highly enriched uranium (HEU)-downblend and partially filled cylinders, but they were not included in the predictions of performance for the NDA methods on the premise that the potential of the NDA methods first needs to be understood for the cylinder types most likely to be encountered in IAEA verification scenarios (i.e., ore-based NU feed and cylinders filled to their maximum weight capacity).

Figure 17 displays the assay results for the traditional enrichment meter method implemented using the square-wave convolute (SWC) algorithm for the extraction of net peak count rate for the 3.8 cm × 3.8 cm $LaBr_3$ and the 7.6 × 7.6-cm NaI spectrometers, with the Fe/poly collimator/converter design. The SWC algorithm is discussed in an Appendix (Section 6). The live times were 400 seconds for the $LaBr_3$ and 300 seconds for the NaI. The one-sigma error bars in these plots reflect only the statistical counting uncertainty in the net peak count rate, and not the systematic uncertainty in the fitting algorithm. This statistical uncertainty is significantly less than the overall standard deviation for nearly all of the cylinders, as expected, since systematic uncertainties such as wall-thickness variation and nonlinear continuum subtraction are generally the largest source of uncertainty in the traditional enrichment-meter approach.

The relative standard deviations from the declared [235]U enrichments for the 23 product cylinders are 3.1% for $LaBr_3$ and 3.5% for NaI; for the two natural-enrichment cylinders, 9.4% for $LaBr_3$ and 7.9% for NaI; for the depleted cylinders, 11% for $LaBr_3$ and 13% for NaI. The $LaBr_3$ and NaI performance is comparable over the entire enrichment range (0.2 to 5.0 wt% [235]U), but the number of natural and depleted cylinders is very limited.

While the Fe/poly collimator design is the more appropriate for a hybrid enrichment assay station also collecting the non-traditional signature, comparison with the results from the lead collimator design used in the April 2010 measurements (Prototype #2a) indicates how the traditional enrichment meter performance is compromised by using a collimator designed to enhance the non-traditional signature. For the lead collimators, the relative standard deviations from the declared [235]U enrichments for the 16 product cylinders are 3.2% for $LaBr_3$ and 3.8% for NaI. As with the Fe/poly case, the $LaBr_3$ and NaI performance is comparable and the performance difference between the two collimator configurations is relatively small.
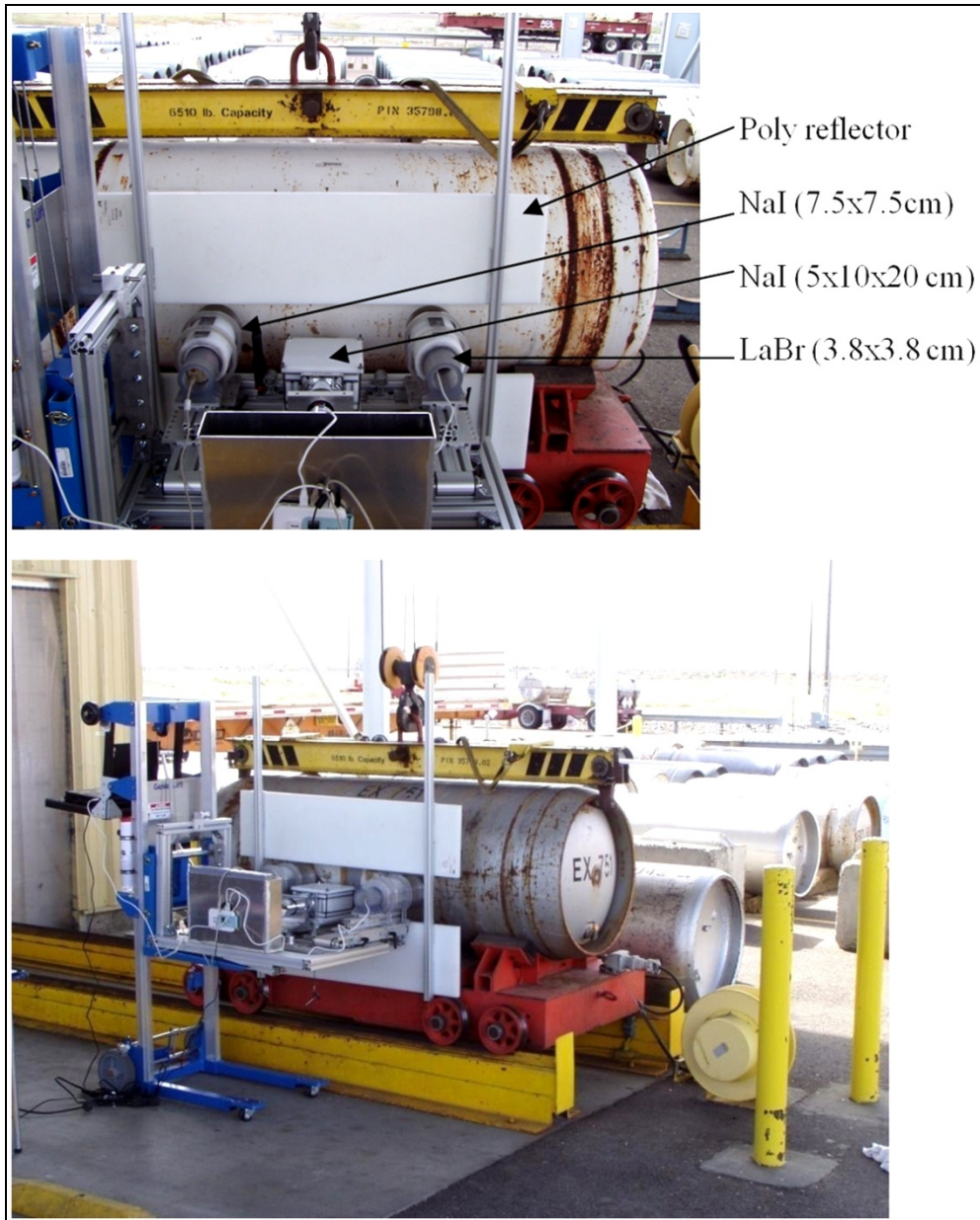
Figure 15. Photographs of sensor package and measurement setup at AREVA NP fuel fabrication facility for May 2010 field campaign.
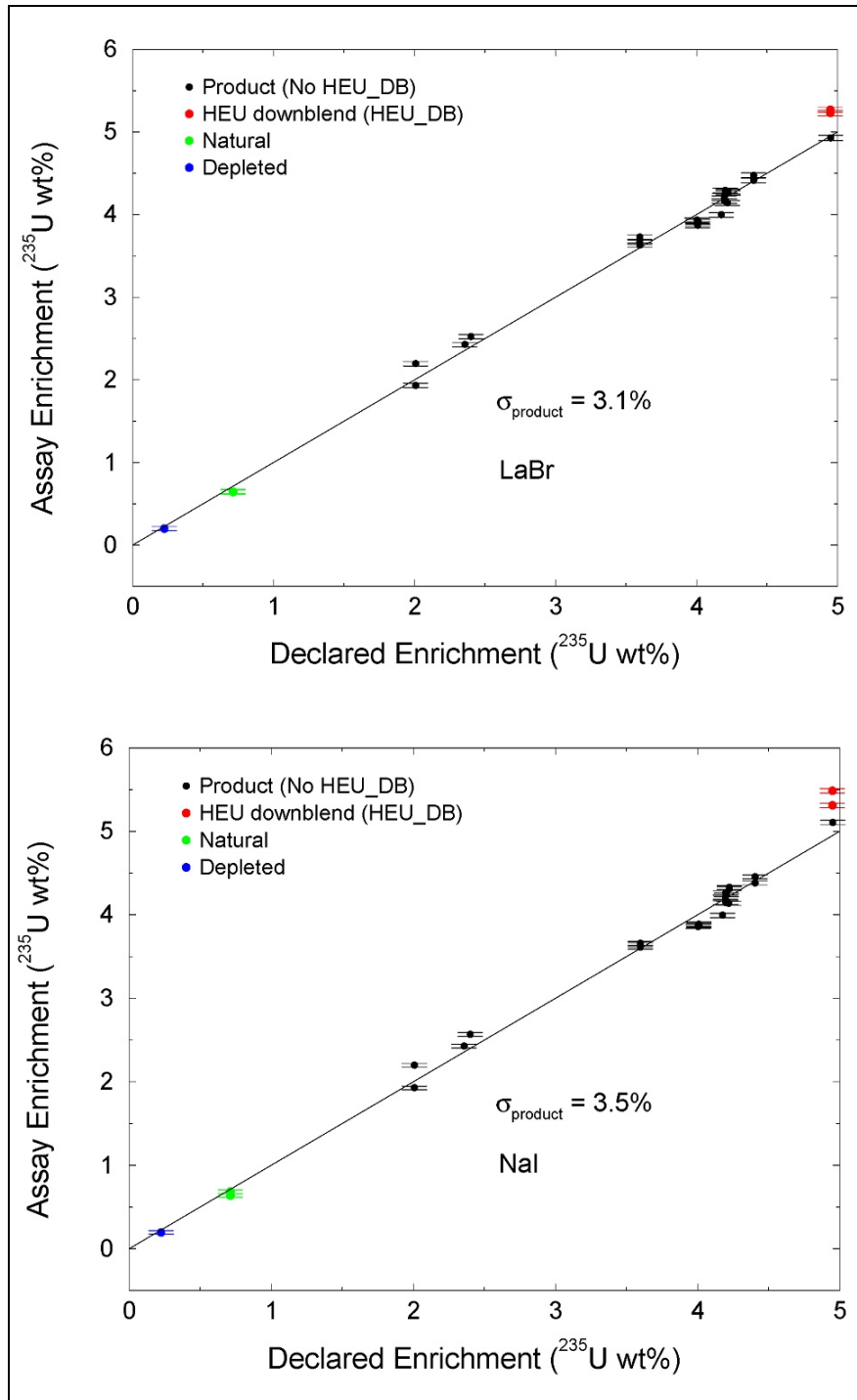
Figure 16. Assay enrichment versus declared enrichment using the traditional enrichment-meter method and a square-wave convolute algorithm for the calculation of net count rate in the 186-keV peak, May 2010 AREVA field campaign data: LaBr$_3$ (Top) and NaI (Bottom). The analysis data set spans 26 full cylinders (0.2 to 5 wt % ^{235}U) but does not include the HEU down-blend cylinders (red data points). The one-sigma error bars reflect only the statistical counting uncertainty in the assay enrichment.

Table 4-3 summarizes results for the traditional, non-traditional and hybrid enrichment analyses, and compares it to AREVA's assay using a fixed-geometry HPGe system and the traditional enrichment-meter method. The AREVA cylinder verification system is an important point of comparison because it represents best-case performance for an attended (due to need for cryogenic cooling) NDA system. Achieving comparable or improved performance using the hybrid methods, suitable for an unattended system, would be highly desirable.

Table 4-3. Summary of enrichment assay results for a population of 26 Type 30B cylinders: 23 product (greater than 2.0 wt% ^{235}U), 2 natural, and 1 depleted, May 2010 AREVA field campaign. Results are given in terms of relative standard deviation from the declared enrichment values.

Method	Product	Natural	Depleted
Approximate Target Uncertainty [Kuhn 2001]	**5**	**10**	**15**
Traditional HPGe (from AREVA)	**3.3**	**5.2**	**12**
Traditional LaBr$_3$ (SWC method)	3.1	9.4	11
Traditional NaI (SWC method)	3.5	7.9	13
Non-Traditional NaI	3.7	4.9	32
Hybrid NaI (simple average)	**2.5**	**4.6**	**9.7**

May 2011

Based upon the field data collected at AREVA with the 2010 Prototype #2 (Figure 16) sensor package, we concluded that a sensor package consisting of three 7.6 cm × 7.6 cm cylindrical NaI detectors would suffice to measure the traditional assay signature without requiring a more expensive LaBr$_3$ or a larger NaI detector in cylindrical or log geometry. Detector modeling indicated that 7.6 cm × 7.6 cm NaI detectors outfitted with pulse-processing and data acquisition electronics of sufficient dynamic range would also provide a good response in the non-traditional, high-energy gamma-ray (3 to 8 MeV) signature region. Comparable performance for the traditional signature between two sets of collimators deployed in the April 2010 campaigns, one optimized for low-energy gamma-ray attenuation and one optimized for conversion of neutrons to gamma-rays for the nontraditional signature, suggested that collimation tailored for the nontraditional signature could be confidently applied to spectrometers collecting data for either signature. To test these expectations, PNNL deployed a third modification ("Prototype #3") of the portal sensor package in a field campaign at AREVA in 2011. The third-generation sensor package comprised an array of three cylindrical NaI spectrometers (7.6 cm diameter × 7.6 cm length) sheathed in modeling-optimized collimators; see Figure 18 and Figure 19. Measurement live times were 600 seconds per cylinder. The modeling process used to optimize the collimation design is discussed in Section 3 above. An important measurement objective in

the 2011 campaign was to demonstrate effective collection of both traditional and non-traditional signature data using the same array of NaI spectrometers.
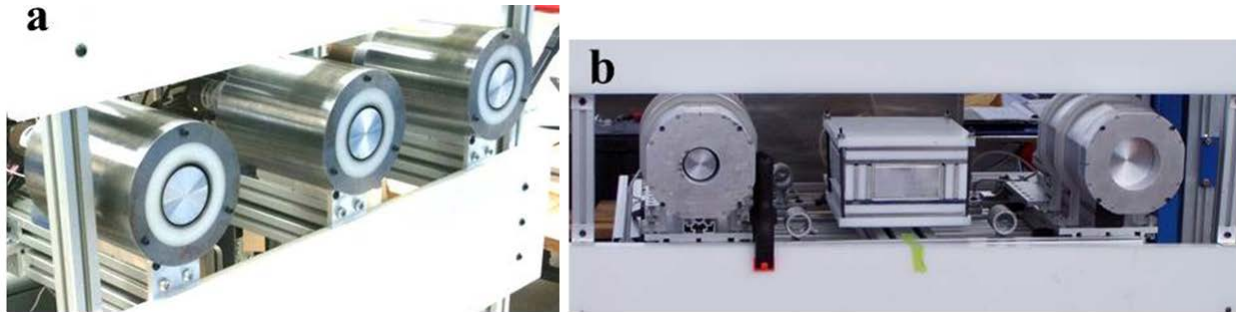

Figure 17. Comparison of spectrometer packages deployed in 2011 (a) and 2010 (b) field campaigns at AREVA. (a) Optimized collimators on field Prototype #3 (May 2011) with three 7.6 cm × 7.6 cm NaI detectors sheathed in modeling-optimized collimators, (b) previously-deployed field Prototype #2 with (from left to right) a 3.8 × 3.8 cm LaBr$_3$ detector, a 5 ×10 × 20 cm^3 NaI(Tl) detector and a 7.6 cm × 7.6 cm NaI detector.

Figure 18. Photograph of experimental setup at AREVA fuel fabrication facility using the sensor package Prototype #3, May 2011 field measurement campaign.

We studied the non-traditional gamma-ray yield as a function of collimation. Table 4-4 compares net count rates in the non-traditional signature (3-8 MeV) region for three cases: 1) modeled results in the Prototype #3 configuration (May 2011, three 7.6 cm × 7.6 cm NaI spectrometers with optimized Fe/poly collimation), 2) measured data from AREVA using the Prototype #3 configuration, and 3) measured data from the 2010 AREVA field campaign with the Prototype #2b configuration (5 × 10 × 20 cm^3 NaI log spectrometer, Fe/poly collimation). The measured yield from the sum of the three NaI spectrometers matches the yield from the NaI

log to within about 1.5% for a typical LEU product cylinder, indicating that the array of smaller scintillation spectrometers with optimized collimation is an adequate replacement for the larger, more expensive NaI log-form factor detectors. The simulated sensor response reproduces the measured data in the high-energy gamma-ray region to within about 13%. The fact that the simulation currently underpredicts the measured response may be symptomatic of infidelities in the model of environmental neutron moderation, or it may reflect uncertainties in the background subtraction procedure required to extract the net high-energy yield in the measured data.

Table 4-4. Comparison of non-traditional, high-energy gamma-ray responses for May 2011 (sensor package Prototype #3) and May 2010 (Prototype #2). Modeling-optimized Fe/Poly collimation has been incorporated for the Prototype #3 configuration, and the form factor of the NaI detector changed, relative to the Prototype #2b configuration. Statistical uncertainties on model and data are of order 0.1% for the LEU count rates.

Collimator Design	Detector Type Modeled/Measured	Net Count Rate in 3-8 MeV Region (cps)		
		LEU (~5%)	Natural (0.71%)	Depleted (0.20%)
Prototype #3	Three 7.6 cm × 7.6 cm NaI (sum), Modeled	107	24.6	14.8
Prototype #3	Three 7.6 cm × 7.6 cm NaI (sum), Measured	123	23.8	n/a in May 2011
Prototype #2b	One 5×10×20 cm^3 NaI log, Measured	125	24.7	13.8

Table 4-5 summarizes assay results in the May 2011 AREVA campaign and compares them to the results obtained with the previous incarnation of the sensor package in the May 2010 campaign. (Note that no depleted cylinders were measured in the 2011 campaign; corresponding entries in the table are thus marked "N/A".) The results show that a set of three 7.6 cm × 7.6 cm NaI spectrometers, coupled with modeling-optimized Fe/poly collimators, permit exploitation of traditional and non-traditional signatures with precision comparable to that of larger, more expensive, and/or better energy resolution detector types used in previous prototypes.

Table 4-5. Summary of enrichment assay results for FY2011 (sensor package Prototype #3) and FY2010 (Prototype #2b) measurements of Type 30B cylinders at AREVA NP. Results are given in terms of standard deviation from the declared enrichment values over the cylinder populations assayed.

Method	Product	Natural	Depleted
Approximate Target Uncertainty [Kuhn 2001]	**5**	**10**	**15**
Traditional HPGe (from AREVA), 2010	3.3	5.2	12
Traditional LaBr$_3$ (SWC method), 2010	3.1	9.4	11
Traditional NaI (SWC method), 2010	3.5	7.9	13
Non-Traditional NaI, 2010	3.7	4.9	32
Hybrid NaI, 2010 (simple average)	**2.5**	**4.6**	**9.7**
Traditional HPGe (from AREVA), 2011	3.2	5.0	N/A
Traditional NaI (SWC method), 2011	4.9	7.4	N/A
Non-Traditional NaI, 2011	2.9	7.6	N/A
Hybrid NaI, 2011 (simple average)	**2.7**	**5.6**	**N/A**

5.0   Summary and Future Development

Proof-of-principle research results obtained to date suggest the feasibility of meeting IAEA precision standards for enrichment assay of product, feed, and depleted UF$_6$ contained in 30B cylinders using a sensor package deployed in a "portal monitor" form-factor. Although all measurement campaigns conducted to date have involved attended data collection on relatively small populations of cylinders, the end-goal of the research is to facilitate deployment of the technology for unattended assay of 100 percent of an enrichment facility's product cylinder stream. The assay method investigated exploits a hybrid measurement and analysis of two passive ionizing-radiation signatures of [235]U content: The traditional enrichment meter method, implemented by spectroscopic analysis of the 186-keV peak, and a non-traditional, high-energy gamma-ray signature generated by interaction of neutrons emitted from the UF$_6$ with proximate materials (e.g. steel in the cylinder walls, and the scintillation spectrometer itself in the case of NaI).

We have tested several incarnations of the detector package over the course of the research lifecycle, with the general objective of minimizing complexity and cost of the spectrometer instrumentation while retaining (and, to the extent possible, enhancing) assay precision:

- Prototype #1: Distinct neutron sensors (i.e. He-3 tubes in a moderator matrix) and relatively large, medium-resolution gamma-ray spectrometers (i.e. NaI "logs"), deployed in measurements aimed at testing the proportionality of the neutron emission rate to the

U-235 mass (requiring, in turn, a stable isotopic abundance ratio of U-234 to U-235) and demonstrating correlation of the high-energy gamma-ray response to the neutron response;

- Prototype #2: Gamma-ray spectrometers only, consisting of a mix of collimated spectrometers (NaI and LaBr3) for measurement of the traditional signature, in combination with a large NaI spectrometer log dedicated to measurement of the high-energy signature;
- Prototype #3: An array of three identical gamma-ray spectrometers (NaI) in collimation optimized for registering the nontraditional signature (i.e. moderation and conversion of neutrons in the vicinity of the detectors) while preserving sufficient attenuation at 186-keV to effectively implement the traditional enrichment meter method at several locations on the inspected cylinder.

The most important performance results to date are summarized in Table 4-5 above. We conclude the following on the basis of cylinder populations measured at the AREVA enrichment facility in Richland, WA:

- The hybrid assay approach, implemented using a sensor package of only relatively modest design complexity and cost (i.e. three 7.6 cm × 7.6 cm NaI spectrometers sheathed in appropriate collimation consisting of steel and polyethylene), offers an assay precision for LEU product cylinders (enrichment in the range of 2 wt% to 5 wt%) below 3%. This comfortably satisfies an approximate IAEA target specifications for assay precision [Kuhn 2001] of 5%.
- We have demonstrated hybrid-signature assay precision with the same prototype sensor for 30B cylinders containing natural uranium feed (5.6%). This also satisfies the approximate 10% target precision established by the IAEA.
- No depleted-cylinder measurements have been carried out with the Prototype #3 incarnation of the sensor. Measurements on a limited set of depleted cylinders using the previous prototype (i.e., cylindrical NaI, cylindrical LaBr$_3$, log NaI) suggest an assay precision of about 10%, again comfortably satisfying the IAEA target (15%).
- Data collected during the FY-2010 AREVA field campaign suggest that applying a facility-specific, and possibly feed-source specific, calibration of the non-traditional signature will have a marked effect (amounting to roughly a 1 part in 4 improvement) on the assay precision achievable with the hybrid method. This dependence arises from the requirement of a stable ^{234}U/^{235}U ratio in correlating neutron yield from the UF$_6$ with ^{235}U mass.
- Measurement times per cylinder in field campaigns to date are in the range 5 to 10 minutes. For these collection times, uncertainties from Poisson counting statistics are typically an order of magnitude smaller than the observed dispersion in assayed enrichment relative to declared values.

Future development of the hybrid-signature assay approach will emphasize more thorough characterization of the potential assay precision for all relevant external-stream UF$_6$ enrichments

and development of automated procedures and algorithms appropriate for an unattended portal station. The FY-2010 and FY-2011 field campaigns at AREVA suggest that a hybrid assay method can meet target uncertainties for LEU and natural enrichments. To date we have carried out only a very few measurements on depleted uranium cylinders, however, and none with the current multi-NaI sensor array form factor. In addition, all of our measurements have been based upon Type 30B cylinders, rather than the Type 48 cylinders that are the industry standard for feed and tail material. A more definitive assessment of the viability of the hybrid NDA methods for product, tail and feed cylinders will require an extended measurement campaign at an operating enrichment plant. Such a campaign should utilize an array of NaI spectrometers and an accompanying suite of collimator/converters, pulse-processing electronics and enrichment analysis algorithms specifically tailored to the hybrid NDA methods.

Ongoing project activity in FY-2012 is exploring this possibility. We anticipate that the HEVA will be deployed to a nuclear facility, such as a Gas Centrifuge Enrichment Plant (GCEP), to measure a large selection of enriched, depleted and natural uranium filled cylinders. This effort is part of Action Sheet 40 between the U.S. Department of Energy and the European Atomic Energy Community (EURATOM).   Action Sheet 40 provides for the exchange of recent findings by the U.S. and EURATOM on NDA methods for UF_6 cylinder verification and execution of a joint measurement campaign that would result in the collection of data with selected detection systems on product, tail, and feed cylinders at an enrichment facility. The objective of this work is to promote and advance the capabilities of both parties in the area of cylinder verification. The data collected during the measurement campaign will characterize the capabilities of more mature NDA technologies and guide the research and development of future NDA technologies used to verify nuclear material contained in UF_6 cylinders. The results of the survey and field test will be described in a technical report and made available to the IAEA. The location of the measurement campaign has yet to be determined.

In keeping with a graded approach to instrument development and testing, PNNL will continue to pursue the possibility of further field campaigns at the AREVA fuel fabrication plant in Richland, Washington as a convenient and cost-effective location for testing and evaluation of both hardware design options and algorithm variants. AREVA receives new shipments of Type-30B cylinders on a regular basis, with a range of enrichments from depleted (0.2%) to 5%, and we may be able to measure upwards of 200 Type-B cylinders in a few months. Importantly, the AREVA cylinder population comes from a variety of enrichment providers (e.g., URENCO, USEC, Ural) so that we may more fully investigate some of the systematic sources of uncertainty that might arise from different enrichment processes.   Design and fabrication of a 4th-generation sensor package comprising four collimated NaI spectrometers and a supporting cart (see Figure 19) appropriate for deployment in both measurement campaigns noted above is underway in FY-2012.

Optimization, automation, and systematic uncertainty characterization of the analysis algorithms used to implement the hybrid-signature assay approach are also a subject of ongoing study. Data

reduction of field measurement campaigns to date has enjoyed the advantage of expert-supervised data inspection and interpretation. Developing automated implementations of the analysis algorithms (discussed briefly in the Appendix below) and evaluating the potential performance of these algorithms in an unattended portal represent key challenges to the migration of the technology from field-testing to practical deployment. We are currently studying possible alternatives to the digital-filter peak-area extraction method adopted for analysis of the 186-keV region in the FY-2010 and 2011 field campaigns, with an eye toward understanding the robustness against systematic effects (e.g. gain drifts in the NaI spectrometers) and the potential assay precision of these candidate methods. We are similarly quantifying uncertainties related to detector gain drift for the nontraditional, high-energy gamma-ray method. Finally, we are currently carrying out a modeling-based assessment of the impact of a variety of systematic uncertainties on the hybrid assay technique. Potentially important sources of uncertainty include variations in wall-thickness, UF_6 fill profile, material age and U-234/U-235 ratio, and temporal variations in facility ionizing-radiation backgrounds arising from changes in proximate cylinder locations.
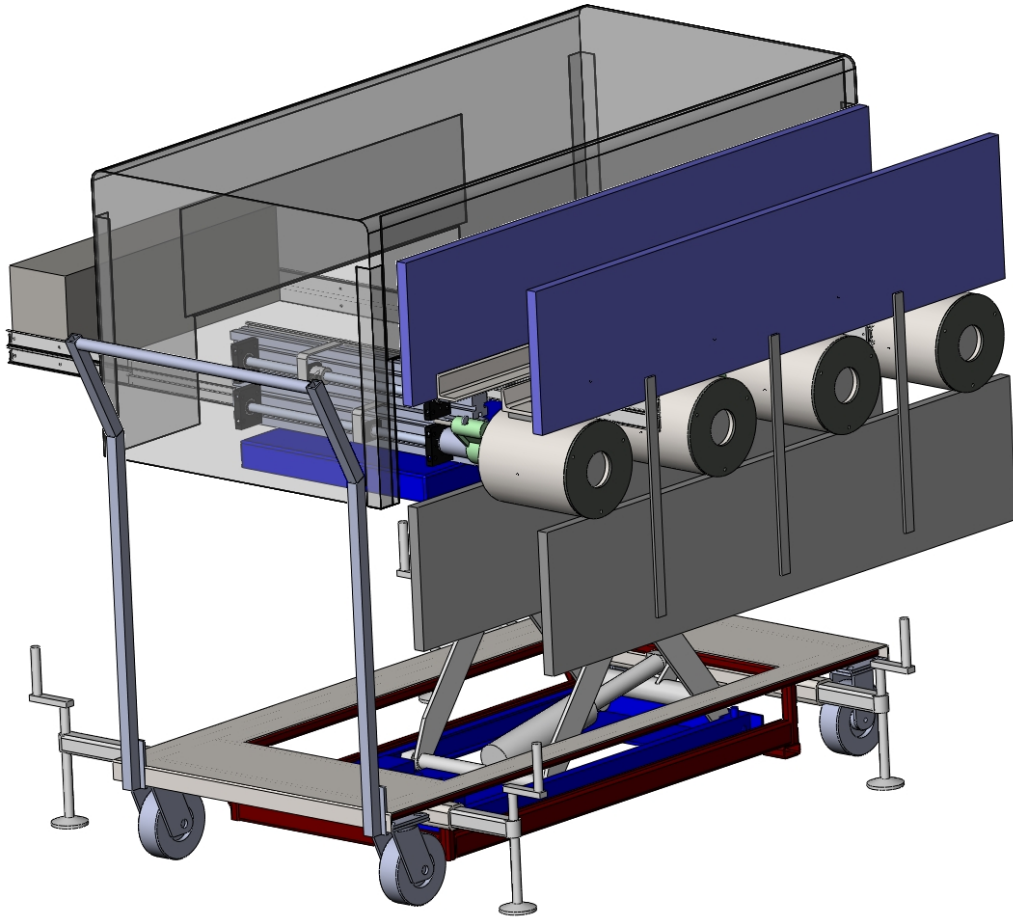
Figure 19. Conceptual illustration of the FY-2012 incarnation of the HEVA sensor package and supporting cart currently being fabricated at PNNL.

6.0   Acknowledgements

7.0   Appendix: Analysis Methods

This appendix touches briefly upon some of the spectrum-analysis and enrichment assay calibration methods adopted for data reduction in the various field campaigns discussed in the main body of the text. In general, an overarching theme of the development of these techniques is the potential difference in robustness and assay precision between analyst-supervised and unattended, automated application domains. Ultimately we wish to adapt the methods described here for unsupervised use in a facility-deployed cylinder assay portal. Most of the analytical work conducted to date, however, has emphasized "eyes-on" application of candidate analysis algorithms and procedures. This is partly of necessity, because the form factor and spectrometer sets comprising the various prototype sensor packages have been in flux over the history of the research. However, ongoing and future work will begin to focus on a stable package design and a relatively fixed deployment scenario (perhaps with particular automated data acquisition frameworks or protocols to serve as constraints upon the data and analysis flow), and we will turn more serious attention to the automation of the analysis methods.

Implementing the traditional enrichment meter method requires analysis of the 186-keV peak region to extract the area under the peak. Several possible approaches to peak area determination are possible. The spectroscopic analysis algorithm adopted for the current work involves application of a discrete form of a so-called zero-area digital filter, the *square-wave filter* [Op de Beeck 1975, Janssens 1991], to the pulse-height spectra collected with the NaI spectrometers. We refer to the convolution of the original spectrum with the digital filter as the "square wave convolute" (SWC) spectrum. A key property of any symmetric, zero-area digital filter is that by construction, it removes background components varying linearly with energy.   Figure 20 (left panel) illustrates the shape of the square-wave filter, *g(t)*, which is fully described by a single width parameter, *M*. The variable *t* labels channel number in the pulse-height spectrum. Figure 20 (right panel) illustrates the effect of applying the square-wave filter to a simple "toy" spectrum consisting of a pure Gaussian peak superimposed on a linear background. This example highlights key qualitative features of the convolute spectrum:

- The linearly-varying background portion of the raw spectrum is effectively filtered out, yielding a flat baseline.
- The original Gaussian peak in the raw spectrum is replaced by a characteristic peak-shape comprising a positive-going central peak region plus negative-going side "troughs". The position of the central peak of the convolute spectrum coincides with the position of the Gaussian in the original spectrum. The positions of the two side-troughs roughly demarcate the points in the original spectrum at which the Gaussian peak returns to the level of the linear continuum in the raw spectrum.
- The amplitude of the peak in the SWC spectrum is proportional to the area under the original Gaussian peak (this proportionality holds strictly only in the absence of nonlinearity, or curvature, in the continuum as a function of energy).
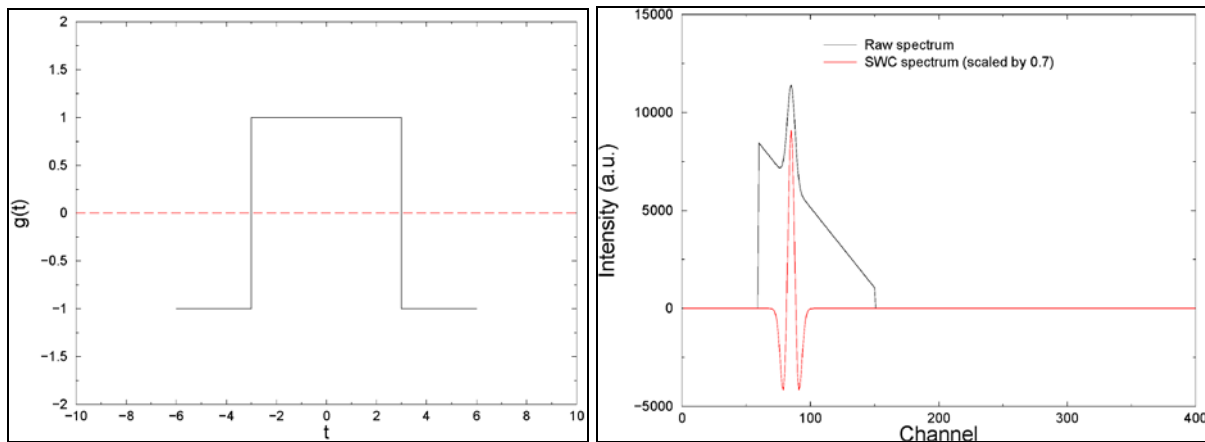

Figure 20. Left panel: Illustration of square-wave filter shape for filter width M = 6. Right panel: Effect of the filter applied to a simple "toy" spectrum consisting of a Gaussian peak superimposed on a linear background.

Although a zero-area digital filter is typically used for peak recognition and interference detection, Op de Beeck [1975] documents efforts to extract peak area information from the amplitude of the SWC peak. In the present application, which aims to develop robust spectrum algorithms for unattended assay of 30B cylinders, the SWC technique offers a potentially attractive peak-area extraction alternative to methods that adopt e.g. nonlinear fitting methods (i.e., Gaussian + polynomial continuum) to model the shape of the spectrum in the region of the 186-keV peak. The location of the prominent peak in the SWC spectrum is easily determined by pattern recognition (see for example Figure 21), so that the method offers robustness against spectrometer gain drift.
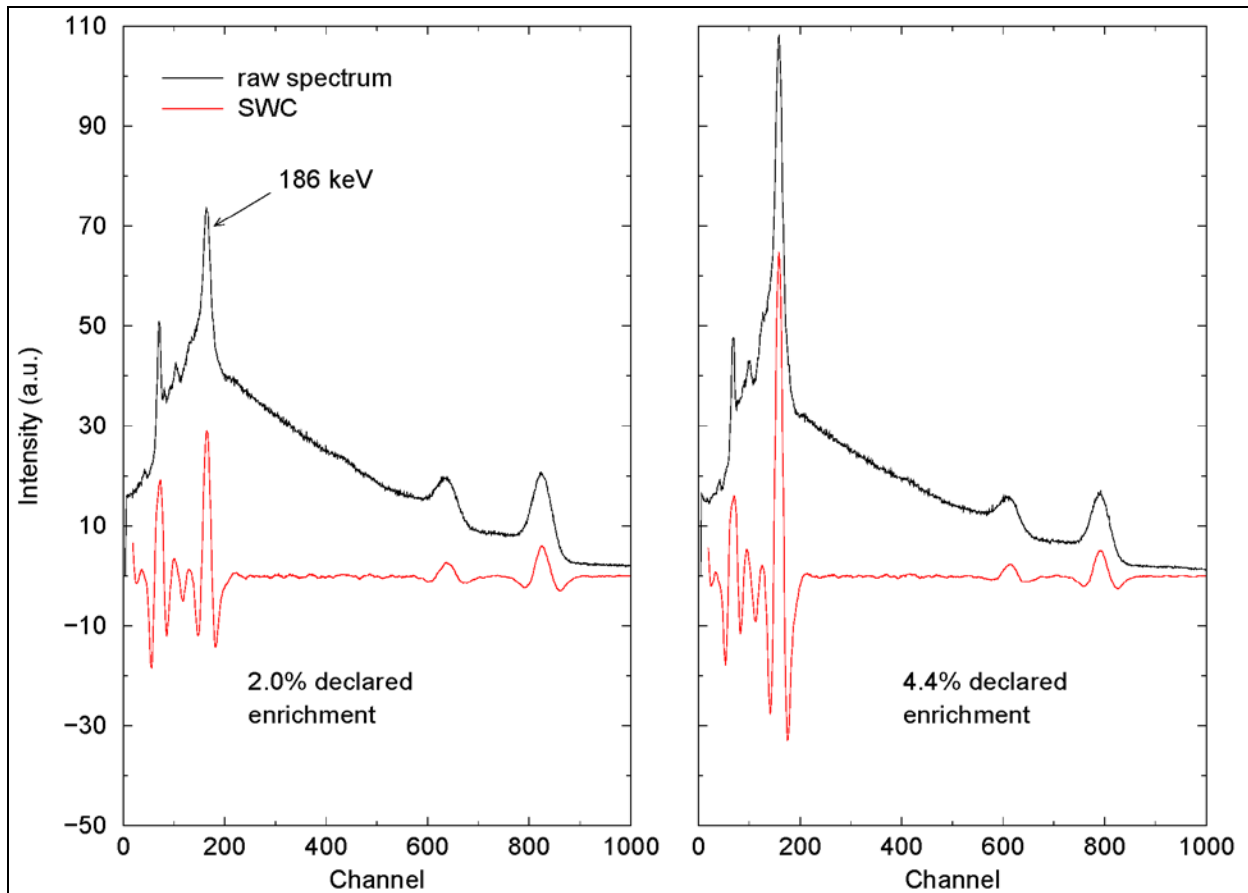
Figure 21. Illustration of the square-wave convolute method on two UF$_6$ spectra recorded from 30B cylinders with a NaI(Tl) spectrometer. Note that application of the digital filter effectively removes the constant and linear components of the underlying continuum. The variation of amplitude in the prominent convolute spectrum peak corresponding to the 186-keV peak in the raw pulse-height spectra suggests the proportionality of the amplitude to the area under the original 186-keV peak.

In brief, the analysis procedure adopted for the field-measurement campaigns conducted to date involves the following steps. (The spectroscopic analysis details have varied somewhat with differing sensor package prototypes and spectrometer types.) For concreteness in describing the spectroscopic analysis, we focus here upon the traditional enrichment method. But the assay calibration procedure adopted for the non-traditional gamma-ray signature (which employs a simple summation over the 3 to 8 MeV region-of-interest in the energy-calibration pulse height spectrum) is very similar.

1. Energy calibration: The channel positions of the 186-keV, 766-keV, and 1001-keV peaks are determined by a "conventional" spectrum analysis approach consisting of a fit to the local peak region with a Gaussian peak + polynomial background function. In this sense, the spectrum analysis procedure applied to the AREVA data is not completely decoupled from conventional fitting techniques, although the energy calibration approach described here could be adapted readily to consume peak positions derived from the convolute spectrum, rather than from fits to the raw spectrum.

32

2. Spectrum analysis: We calculate the SWC spectrum from the raw spectrum. Peaks in the convolute spectrum are identified using a simple crest-above-threshold algorithm that determines the positions (expressed in channel units) of local maxima above a user-specified threshold. Of primary interest in this peak-selection algorithm is the survival of the 186-keV peak as a "candidate" for the next stage of peak identification. With a set of candidate peaks in hand, and the energy calibration as determined in step (1) above, the identification algorithm then determines the peak that most closely matches the energy of the 186-keV peak of interest. The amplitude of the 186-keV convolute peak is then determined simply by recording the convolute value in the peak channel.

3. Assay calibration: For a given spectrometer (or sum over spectrometer responses), we then determine the enrichment calibration by fitting a line to the set of 186-keV convolute peak amplitude values (with associated statistical uncertainties derived from Poisson counting statistics in the raw input spectrum) as a function of the declared enrichment.

4. Cylinder population assay: The enrichment of a sample cylinder relative to the assay calibration curve from an observed convolute peak amplitude is then determined simply by inverting the linear fit obtained in step 3. A similar approach, using the nontraditional signature's high-energy continuum response in the 3 to 8 MeV region of interest, yields an assay on the basis of this signature. The hybrid assay is currently determined simply by computing the arithmetic average of the traditional and nontraditional assays, although more sophisticated weightings of the two contributing signatures can be envisioned.

5. Calculation of cylinder-population assay precision metric: The primary statistical metric adopted in this research to summarize dispersion of the enrichment assay results is the standard deviation of the relative, or fractional, difference of assayed enrichments from declared. In general, this standard deviation may be computed for the same subset, or for a different subset, of the overall population of cylinder measurements used to determine the assay calibration. For example, one may analyze the set of all {product, natural, depleted} cylinder measurements in a given field campaign to determine the calibration curve, and then separate relative standard deviations computed for the product, natural, and depleted sub-populations.

8.0   References

[Dias 2008] F. Dias, E. A. de Luceana, B. R. McGinnis, B. Rollen, and S. E. Smith, "Verification of U-235 isotopic abundance in low enriched UF6 cylinders by a low resolution spectroscopy technique," Proceedings of the 49th Annual Meeting of the Institute of Nuclear Materials Management 2008, Nashville, Tennessee, July 13-17, 2008, Curran Associates, Inc., Red Hook, New York.

[Hensley 2006] W. K. Hensley, "SYNTH: A computer code to generate synthetic Gamma-Ray Spectra," pp. Developed by The Pacific Northwest National Laboratory, Richland, WA, USA, with Government support under Contract Number DE-AC06-76RLO-1830 awarded by the United States Department of Energy. Copyright 1994-2006 Battelle Memorial Institute.

[Janssens 1991] F. Janssens, F and J.P. Francois, "Evaluation of 3 Zero-Area Digital-Filters for Peak Recognition and Interference Detection in Automated Spectral Data-Analysis." Analytical Chemistry 63(4):320-31, 1991.

[Kuhn 2001] E. Kuhn, et al., "International target values 2000 for measurement uncertainties in safeguards nuclear materials," IAEA STR-327, International Atomic Energy Agency, Vienna, Austria, 2001.

[Mace 2010] E.K. Mace and L.E. Smith, "Automated Nondestructive Assay of UF6 Cylinders: Detector Characterization and Initial Measurements." In *NIM A Proceedings (SORMA 2010)*, Article in Press, Available online, 2010. doi:10.1016/j.nima.2010.09.149

[McDonald 2011] B. S. McDonald, Jordan, D.V., Orton, C.T., Mace, E.K., Wittman, R.S., Smith, L.E., "Model and Algorithm Evaluation for the Hybrid UF6 Container Inspection System," *Institute of Nuclear Materials Management Annual Meeting*, (2011).

[Mitchell 2010] D. J. Mitchell, L. T. Harding, and K. R. Smith, "Neutron Detection With Gamma-Ray Spectrometers for Border Security Applications," *IEEE Transactions on Nuclear Science,* vol. 57, no. 4, pp. 2215-2219, 2010.

[Op de Beeck 1975] J. Op de Beeck, "Gamma-Ray Spectrometry Data-Collection and Reduction by Simple Computing Systems." *Atomic Energy Review* 13(4):743-805, 1975.

[Reilly 1974] T.D. Reilly, E.R. Martin, J.L. Parker, L.G. Speir, and R.B. Walton, "A Continuous In-Line Monitor for UF6 Enrichment," Nucl. Tech., vol. 23, pp. 318-327, 1974.

[Reilly 1991] D. Reilly, N. Ensslin, H. Smith, and S. Kreiner, "Passive nondestructive assay of nuclear materials," NUREG/CR-5550, LA-UR-90-732, U.S. Nuclear Regulatory Commission, Washington, D.C., 1991.

[Richter 1999] S. Richter, A. Alonso, W. De Bolle, R. Wellum, and P. D. P. Taylor, "Isotopic "fingerprints" for natural uranium ore samples," Int. J. Mass Spectrom., vol. 193, no. 1, pp. 9-14, 1999.

[Smith 2009] L.E. Smith, M.M. Curtis, M.W. Shaver, J.M. Benz, A.C. Misner, E.K. Mace, D.V. Jordan, D. Noss, and H. Ford. "Development of a Portal Monitor for UF6 Verification." In *Proceedings of the 50th Annual Meeting of the Institute of Nuclear Materials Management*. Institute of Nuclear Materials Management, Deerfield, IL. 2009.

[Smith 2010a]   L.E. Smith, D.V. Jordan, A.C. Misner, E.K. Mace, and C.R. Orton. "Hybrid Enrichment Assay Methods for a UF6 Cylinder Verification Station." In *Proceedings of the 51st Annual Meeting of the Institute of Nuclear Materials Management.* Institute of Nuclear Materials Management, Deerfield, IL. 2010.

[Smith 2010b]   L.E. Smith, E.K. Mace, A.C. Misner, and M.W. Shaver, "Signatures and Methods for the Automated Nondestructive Assay of UF6 Cylinders at Uranium Enrichment Plants." *IEEE Transactions on Nuclear Science*, vol. 57, no. 4, pp. 2247-2253, 2010.

[Smith 2012] L.E. Smith, A. Lebrun, D. Beddingfield, "Potential Roles for Unattended Instrumentation at Enrichment Plants," Presentation at the GCEP Technology Stakeholders Meeting held at the University of Virginia, Charlottesville, VA, 17 May 2012.

[Walton 1974] R. B. Walton, T. D. Reilly, J. L. Parker, J. H. Menzel, E. D. Marshall, and L. W. Fields, "Measurements of UF6 Cylinders with Portable Instruments," Nucl. Tech., vol. 21, no. 2, pp. 133-148, 1974.

[Wilson 2005] W. Wilson, R. Perry, W. Charlton, T. Parish, and E. Shores, "SOURCES: a code for calculating (a, n), spontaneous fission, and delayed neutron sources and spectra," Radiation protection dosimetry, vol. 115, no. 1-4, pp. 117, 2005.